

White matter changes in mild cognitive impairment and AD: A diffusion tensor imaging study[☆]

David Medina^a, Leyla deToledo-Morrell^{a,b}, Fabio Urresta^{a,1}, John D.E. Gabrieli^{a,e},
Michael Moseley^f, Debra Fleischman^{a,d}, David A. Bennett^{a,d},
Sue Leurgans^a, David A. Turner^c, Glenn T. Stebbins^{a,*}

^a Department of Neurological Sciences, Rush University Medical Center, 1725 W. Harrison, Suite 309, Chicago, IL 60612, USA

^b Department of Psychology, Rush University Medical Center, Chicago, IL 60612, USA

^c Diagnostic Radiology, Rush University Medical Center, Chicago, IL 60612, USA

^d Rush Alzheimer's Disease Center, Rush University Medical Center, Chicago, IL 60612, USA

^e Department of Psychology, Stanford University, Palo Alto, CA, USA

^f Department of Radiology, Stanford University, Palo Alto, CA, USA

Received 8 June 2004; received in revised form 2 August 2004; accepted 30 March 2005

Available online 7 July 2005

Abstract

Diffusion tensor imaging (DTI) can detect, *in vivo*, the directionality of molecular diffusion and estimate the microstructural integrity of white matter (WM) tracts. In this study, we examined WM changes in patients with Alzheimer's disease (AD) and in subjects with amnesic mild cognitive impairment (MCI) who are at greater risk for developing AD. A DTI index of WM integrity, fractional anisotropy (FA), was calculated in 14 patients with probable mild AD, 14 participants with MCI and 21 elderly healthy controls (NC). Voxel-by-voxel comparisons showed significant regional reductions of FA in participants with MCI and AD compared to controls in multiple posterior white matter regions. Moreover, there was substantial overlap of locations of regional decrease in FA in the MCI and AD groups. These data demonstrate that white matter changes occur in MCI, prior to the development of dementia.

© 2005 Elsevier Inc. All rights reserved.

Keywords: Aging; Cognition; Dementia; Fractional anisotropy; MRI

1. Introduction

Mild cognitive impairment (MCI) may be a transitional state between normal aging and Alzheimer's disease (AD). Individuals with amnesic MCI differ from healthy elderly in their level of cognitive function, performing more poorly than controls on measures of memory. Despite impaired memory performance, individuals with MCI do not meet diagnostic criteria for dementia [10,43,59–61]. MCI is associated

with a significantly increased risk of developing AD compared to the elderly population without cognitive impairment [14,23,59–61]. Neuropathological and neuroimaging studies report no significant difference in entorhinal volume [26,29] or the extent of cell loss in layer II of the entorhinal cortex [49] in individuals with cognitive complaints and in patients with MCI compared to those with a diagnosis of AD. Since the entorhinal cortex is one of the earliest sites of pathology in AD, these results indicate that patients with MCI may be in the incipient phase of the disease process. Thus, studies of individuals with MCI provide a unique opportunity to investigate prodromal AD.

Structural magnetic resonance imaging (MRI) techniques have been extensively used to investigate the pathophysiology of Alzheimer's disease (AD) *in vivo*. Additionally, individuals with MCI are now being studied in order to identify

[☆] This research was supported by grants AG09466, AG10161 and AG17917 from the National Institute on Aging, National Institutes of Health.

* Corresponding author. Tel.: +1 312 563 3854; fax: +1 312 663 4009.

E-mail address: gstebbin@rush.edu (G.T. Stebbins).

¹ Present address: Department of Psychiatry, Chicago Medical College, Chicago, IL, USA.

anatomical changes that precede a clinical diagnosis and to develop sensitive *in vivo* markers that may be predictive of conversion to AD. The major emphasis of these studies has been on the detection of atrophy in regions of interest known to be pathologically involved in the disease process. Mesial temporal lobe structures critically important for memory function, such as the hippocampal formation and the entorhinal cortex, have received special attention in these investigations [13,21,22,26–30,41,42,47,48,73] because a disturbance in the acquisition of new information is a hallmark of MCI and AD [26,27,29,47,48].

Although most imaging studies of MCI and mild AD have focused on gray matter alterations, a number of post-mortem investigations have documented white matter pathology associated with AD [18,19,31,44,45]. White matter changes associated with AD may reflect different underlying causes or mechanisms. First, white matter changes in AD may be indicative of anterograde Wallerian degeneration, especially in regions close to cortical areas with the greatest pathological burden. Secondly, there may be white matter rarefaction [31] with axonal damage and gliosis. This type of change is diffuse, does not follow the regional extension of pathologically involved gray matter, and may be vascular or ischemic in origin. Third, it has recently been suggested that myelin breakdown is an important component of the disease process in AD [4–6]. According to this hypothesis, damage to oligodendrocytes may be a critical initiating step in the disease. Furthermore, since late developing oligodendrocytes may be more vulnerable, late-myelinating association areas are predicted to be more susceptible to myelin breakdown.

The results of imaging studies tend to support post-mortem findings of white matter abnormalities in MCI and AD. Increased white matter hyperintensities (WMH) have been found in both MCI and AD using either semi-quantitative radiologic ratings scales [2,51] or quantitative measurements [5,12,24,32]. The role of WMH in the pathology or disease severity of MCI or AD is not established, however. Independence between WMH and diagnosis or cognitive impairment has been reported by some authors [12,40,51], while others report significant correlations between WMH and diagnosis or cognitive impairment [2,24,32]. These discrepancies may be due to differences in the sample studied, analytic methods, or sensitivity of the MRI methodology.

A recently developed structural MRI technique, diffusion tensor imaging (DTI), provides increased sensitivity to alterations in the microstructure of white matter *in vivo* and is especially indicative for diseases causing axonal damage and demyelination [7–9,52,70]. DTI detects microstructural alterations in white matter by measuring the directionality of molecular diffusion (fractional anisotropy: FA). Highly organized white matter tracts have high FA because diffusion is highly constrained by the tract's cellular organization. As white matter is damaged, FA decreases due to decreased anisotropic diffusion.

Previous investigations of white matter changes in AD or MCI using diffusion weighted MRI have reported

changes in mean diffusivity and anisotropic diffusion [15,16,33,36,37,39,46,64,65,74]. Most of these studies have been based on analyses of a priori defined regions of interest. The exact regions of alterations in diffusivity or anisotropic diffusion vary between studies, with some reporting greater anterior differences (e.g. [15]) in AD, while others demonstrate posterior or temporal lobe changes in AD and MCI [33,39,46,64,65].

These conflicting results from prior studies may be due to multiple causes such as differences in sample composition (e.g., mild versus moderate cognitive impairment in AD; amnesic MCI versus MCI involving other cognitive domains), imaging technique (diffusion weighted [16,36,37,46,65] versus diffusion tensor imaging [15,33,39,64,68,74]) or location of brain regions chosen for examination of MRI differences. Most studies used a “region-of-interest” (ROI) approach to examine MRI differences between groups. This approach can be subjective with inconsistent definitions of anatomical borders across studies [20] and poor reproducibility [3]. Even when applied by trained individuals with established reliability and reproducibility, differential regional placement of ROIs across studies could contribute to inconsistent reports of differences in DTI indices.

Whole-brain, voxel-based methods applied to the analysis of DTI differences between samples provide a global and comprehensive assessment un-complicated by the potential biases of ROI approaches. These techniques are automated and, therefore, are not subject to issues of human based tracing reliability and/or reproducibility. In addition, voxel-based analyses assess regional changes in DTI parameters independent of a priori constraints and may reveal differences that are not encompassed by specific ROIs.

In the present study, we examined white matter changes in patients with probable mild AD and in those with amnesic MCI compared to controls using whole-brain, voxel-based analyses. We were especially interested in determining whether patients with MCI who are presumed to be in the pre-clinical phases of AD could be differentiated from elderly controls based on white matter changes. To our knowledge, this is the first investigation to use a whole brain analysis of white matter changes in MCI.

2. Materials and methods

2.1. Subjects

Data reported here were obtained from the following three groups of participants: (1) 21 elderly control subjects (NC) with no cognitive impairment, (2) 16 patients who met criteria for amnesic MCI, and (3) 14 patients diagnosed with mild AD. All participants were recruited from the Rush Alzheimer's Disease Center (RADC, Chicago, IL), the community and the Religious Order Study (ROS), a longitudinal, clinico-pathologic investigation of aging and AD in older

nuns, priests and brothers who have agreed to annual evaluations and to brain autopsy at the time of death [11,58]. To be included in the study, participants had to be 65 years of age or older.

2.2. Clinical work-up and subject selection

All evaluations were carried out by members of the RADCS as previously described [28,72]. Briefly, the evaluation incorporated the Consortium to Establish a Registry for Alzheimer's Disease (CERAD [57]) procedures and included a medical history, neurological examination, neuropsychological testing, informant interview and blood tests. The MRI scans of all participants in the present study were reviewed by a neuroradiologist to assess the presence of stroke or other exclusionary brain abnormalities. The clinical diagnosis of probable AD followed NINCDS/ADRDA guidelines [53]; it required a history of cognitive decline and neuropsychological test evidence of impairment in at least two cognitive domains, one of which had to be memory.

Participants diagnosed with MCI underwent the same standard clinical evaluation as the patients with AD, were found to have a deficit in memory only, but did not meet criteria for dementia. Exclusion criteria for both patients with mild probable AD and MCI were evidence of other neurologic, psychiatric or systemic conditions that could cause cognitive impairment (e.g., stroke, tumor, alcoholism, major depression, a history of temporal lobe epilepsy).

Control subjects received the same work-up as the two patient groups. Selection as an elderly control subject required a normal neurological examination, normal cognition and a Mini Mental State Examination (MMSE [34]) score ≥ 27 . Exclusion criteria for the controls were the same as those used for the patient groups. Informed consent was obtained from all participants according to the rules of the Institutional Review Board of Rush University Medical Center.

2.3. Acquisition and processing of MRI data

Scans were performed on a 1.5T GE scanner (General Electric, Milwaukee, WI, USA) equipped with fast gradient Horizon Echospeed upgrades (Rev. 8.4). Single-shot echoplanar diffusion-weighted imaging was used with the following parameters: repetition time, $T_R = 8000$, echo time, $T_E = 97$, gradient duration $\delta = 20$ ms, acquisition matrix 128×128 zero-filled to 256×256 , field of view (FOV) = 240, slice thickness = 6 mm 0 gap, 19 axial slices. Two degrees of diffusion weighting (b values) were used: $b = 0$ and $b = 800$ s/mm². These diffusion weights were applied in six non-collinear directions (xy , yz , xz , $-xy$, $-yz$, $-xz$) with two repetitions of $b = 0$ and four repetitions of each diffusion weighted image. Images were transferred to an off-line workstation (Sun Microsystems, Palo Alto, CA) for processing.

The first step in post-acquisition processing of diffusion tensor-MRI images (DT-MRI) involved the unwarping

of eddy currents. Eddy currents are geometric distortions introduced by the echo planar diffusion weighting gradients and can cause distortions in shear, magnification and/or pixel shifts. A set of CSF nulled inversion recovery images ($T_1 \sim 2100$ ms) are acquired with $b = 0$ as a reference for unwarping eddy current effects in the diffusion weighted images [25,38]. Processing of unwrapped DT images involved the calculation of the six diffusion coefficients defining the six elements of the diffusion tensor [9]. Eigenvectors, defining the three principle directions of diffusion for each voxel were derived from the diffusion tensor. The magnitude of diffusivity in each direction was represented by the eigenvalues for the three eigenvectors. The mean diffusivity (DW) and the fractional anisotropy (FA) were derived from the eigenvalues [7–9]. From this post-processing, three values were constructed for each slice: DW, FA and $b = 0$ ($b = 0$ weighted image = T2 image).

2.4. MRI data analyses

Individual participant slice images for DW, FA and T2 acquisitions were concatenated into whole-brain volumes in acceptable format using software developed by Russ Poldrack, Ph.D. (<http://sourceforge.net/projects/spm-toolbox>). Whole-brain volumes were imported into Statistical Parametric Mapping software [35] (version SPM99) for analysis. To facilitate voxel-by-voxel comparisons between groups, all images were spatially normalized to a standard template. To avoid the geometric distortions associated with diffusion weighted echoplanar imaging, we used the $b = 0$ diffusion weighted (e.g., T2) image obtained during the scanning sequence for normalization. The T2 weighted image was normalized to the standard T2 template in SPM99 using a 12 iteration linear transformation and a non-linear transformation with $7 \times 8 \times 7$ basis functions. The adequacy of transformation of each participant's T2 weighted image to the T2 template was assessed by visual inspection. Parameters from this transformation were then applied to the remaining DT images and statistical maps were created for DW and FA values. This normalization processing re-sampled the volumes into a 2 mm³ voxel size.

To limit our analysis to DW and FA values in white matter, we created individual subject mask volumes that were used to exclude voxels representing white matter abnormalities based on T2 signal, voxels from gray matter, CSF, and extra-cranial space. The first step in creating the masks was to segment the normalized T2 images into CSF, gray matter, and white matter compartments. The segmentation algorithms for defining white matter were based on a probability of greater than 0.80 for white matter classification. This process allowed us to not only exclude voxels from gray matter, CSF and extra-cranial space, but also to exclude areas of white matter in which the T2 signal was altered due to white matter lesions, atrophic changes or other abnormalities on an individual participant basis. Thus, only voxels surviving this threshold were included in the group analyses. The individual white mat-

Table 1
Demographic variables and white matter mask volumes of clinical groups (means \pm S.D.)

	NCI (N=21)	MCI (N=14)	AD (N=14)
Age (years)	77.3 \pm 10.1	78 \pm 5.6	77.4 \pm 6.8
Range	62–96	64–86	70–89
Medians	78.0	78.5	76.5
Education (years)	15.1 \pm 2.0	14.3 \pm 3.3	15.2 \pm 3.2
Female/male	11/10	11/3	9/5
MMSE score	29.3 \pm 0.7	26.9 \pm 2.1*	24.5 \pm 1.9**
Cardiovascular risk factors (%)			
History of myocardial infarction	11.8	0	21.4
Diabetes	5.9	14.3	0
High blood pressure	35.3	35.7	42.9
White matter mask volumes	41015.8 \pm 1255.7	42927.1 \pm 1244.4	44386.9 \pm 949.7

* Significantly different from NCI ($p < 0.001$).

** Significantly different from both NCI ($p < 0.001$) and MCI ($p < 0.001$).

ter masks were then applied to individual subject DW and FA maps. Group differences in voxel level DTI values were assessed using these individual, masked DW and FA maps.

3. Statistical methods

Differences between the three groups of participants in demographic and disease related measures, as well as volumes of white matter masks, were assessed by one-way analyses of variance (ANOVA) followed by post hoc tests (Fisher's). χ^2 -tests were used to determine the relationship between variables such as gender or cardiovascular risk factors, and diagnostic classification.

Voxel-wise group differences in FA and DW were assessed using the ANOVA module in SPM99 followed by group-wise *t*-test comparisons. For these comparisons, significance was determined with a *p*-value of < 0.01 (corrected for multiple comparisons at the cluster level) with a seven-voxel extent threshold.

Determination of the location of voxels demonstrating significantly different DTI values was accomplished by converting the *x*, *y*, *z* coordinates for the peak voxel within a cluster from the Montreal Neurological Institute (MNI) coordinates used in SPM99 analyses, to Talairach coordinates [69] using the MNIToTAL software (<http://www.mrc-cbu.cam.ac.uk/Imaging/mnispace.html>). The resultant Talairach coordinates were entered into a software program that identifies lobar and Brodman area locations [50].

4. Results

Demographic and cognitive status information on the participants is listed in Table 1. Two participants with the diagnosis of MCI were excluded from analyses because of radiologically confirmed cerebral vascular accidents. The age of participants was equitably distributed among the three diagnostic groups [$F(2,46) = 0.02$, $p = 0.974$], with similar medians and ranges. Analyses of independence revealed no

significant relationships between diagnostic groups and variables such as gender ($\chi^2[2] = 2.488$, $p = 0.288$) or the presence of cardiovascular risk factors; i.e. myocardial infarction ($\chi^2[4] = 6.784$, $p = 0.148$), diabetes ($\chi^2[4] = 5.754$, $p = 0.218$) and high blood pressure ($\chi^2[4] = 3.606$, $p = 0.462$) (see Table 1). However, the groups were significantly different on MMSE scores [$F(2,46) = 37.67$, $p < 0.001$]. Pairwise comparisons showed that the control group had significantly higher scores than patients with MCI or AD ($p < 0.001$ for both). Similarly, participants with MCI had significantly higher scores than patients with AD ($p < 0.001$). There were no significant differences in the volumes of the white matter masks between the groups ($F(2,46) = 2.04$, $p = 0.14$).

4.1. Voxel-based comparisons

Voxel-wise comparison for DW failed to reveal reliable group differences. In contrast, voxel-wise analysis of regional differences in white matter FA between the NC, MCI and AD groups using a $p < 0.01$ threshold showed sig-

Table 2
Talairach space-derived distribution of white matter regions with decreased intra-voxel diffusion anisotropy (FA) in MCI subjects compared to age-matched controls

Centroid voxel			Z	Area	Correspondent anatomical location
<i>x</i>	<i>y</i>	<i>z</i> ^a			
−28	−11	17	4.74	405	Left sub-lobar extra-nuclear
−28	−31	8	4.31	20	Left sub-lobar extra-nuclear
16	−19	53	4.23	187	Left frontal lobe sub-gyral
−30	−41	30	3.91	19	Left parietal lobe sub-gyral
−16	−11	45	3.65	21	Left frontal lobe sub-gyral
16	25	37	3.63	21	Right cingulate gyrus
16	16	42	3.48	27	Right cingulate gyrus
28	−15	21	3.44	56	Right sub-lobar extra-nuclear
−20	−7	10	3.41	14	Left sub-lobar extra-nuclear
−16	8	44	3.32	37	Left cingulate gyrus
−22	−47	39	3.1	7	Left parietal lobe sub-gyral
26	20	16	3.08	13	Right frontal lobe sub-gyral

^a Talairach coordinates.

nificant regional group differences. The majority of these were in posterior areas with few regions anterior to the anterior commissure. Approximately 13% of all voxels showing significant differences between the groups were in

anterior regions and the remaining 87% were in posterior regions (12.7% anterior versus 87.3% posterior: $\chi^2[1] = 827$, $p < 0.0001$). NC versus MCI group contrasts revealed significant decrease in FA in the MCI participants in 12 regions

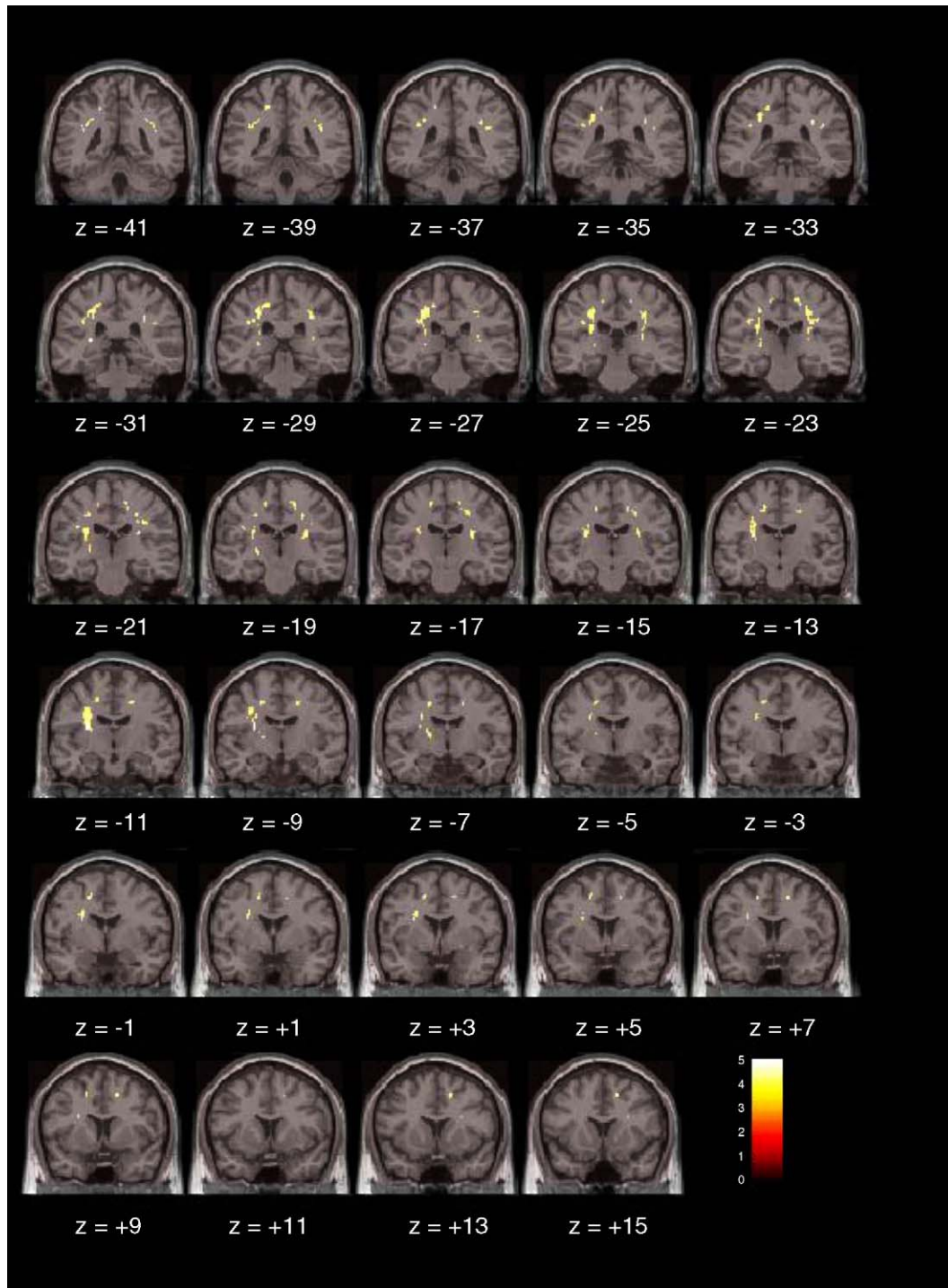


Fig. 1. Representative regions of significantly reduced fractional anisotropy (FA) in patients with mild cognitive impairment (MCI) compared to age-matched healthy control participants. Three dimensional volumes were created from contiguous individual slices and normalized to a common standardized brain volume using SPM99 [35]. Differences were analyzed using a two-sample *t*-test statistic. Significance thresholds were set for $p < 0.01$. Voxels evidencing significant differences between groups are displayed on representative coronal sections on a canonical brain image. The color scale indicates the magnitude of Z values with lowest appearing in dark red and the highest in bright yellow/white. The left side of the images represents the left side of the brain.

Table 3

Talairach space-derived distribution of white matter regions with decreased intra-voxel diffusion anisotropy (FA) in AD subjects compared to age-matched controls

Centroid voxel			Z	Area	Correspondent anatomical locations
x	y	z ^a			
16	21	38	4.26	14	Right cingulate gyrus
16	-19	53	4.06	146	Right superior frontal gyrus
-28	-31	38	4.00	168	Left parietal lobe sub-gyral
-26	-24	22	3.52	51	Left sub-lobar extra-nuclear
-16	8	44	3.49	28	Left cingulate gyrus
38	-42	24	3.47	14	Right parietal lobe sub-gyral
-16	-11	49	3.47	23	Left superior frontal gyrus
-32	-41	28	3.46	8	Left parietal lobe sub-gyral
-22	-45	39	3.20	7	Left parietal lobe sub-gyral
-24	1	28	3.17	32	Left parietal lobe sub-gyral
26	-27	44	3.14	19	Right parietal lobe sub-gyral
26	-25	38	3.12	9	Right frontal lobe sub-gyral
28	-15	21	3.11	42	Right sub-lobar extra-nuclear
32	-8	34	2.75	7	Right frontal lobe sub-gyral

^a Talairach coordinates.

(see Table 2 and Fig. 1). Talairach locations of reduced anisotropy in posterior regions in MCI participants corresponded to the superior longitudinal fasciculus, arcuate fibers underlying the superior frontal gyrus, posterior cingulate bundle, superior and posterior thalamic peduncles, sub-lobar extra-nuclear white matter, and the arcuate fibers of the superior temporal lobe at the temporal-parietal juncture. Anterior regions of decreased FA in the MCI participants were observed in bilateral sub-gyral cingulate gyrus and in the right sub-gyral frontal lobe. There were no regions with significantly increased FA in the MCI compared to NC participants.

Voxel-wise group comparisons of FA differences between NC and AD participants revealed significantly reduced FA in the AD group in 14 regions ($p < 0.01$) (see Table 3 and Fig. 2). Talairach locations of reduced anisotropy in AD compared to NC participants were similar to those found for participants with MCI. Specifically, posterior regions of reduced FA in patients with AD corresponded to the superior longitudinal fasciculus, arcuate fibers underlying the superior frontal gyrus, posterior cingulate bundle, superior and posterior thalamic peduncles, sub-lobar extra-nuclear white matter, and fibers underlying the paracentral lobule. Anterior regions of decreased FA in the AD participants were observed in bilateral sub-gyral cingulate gyrus. There were no regions with significantly increased FA in the AD group compared to NC participants.

To assess the overlap in disturbances of anisotropic diffusion in MCI and AD groups, we examined regions of decreased FA unique to the NC versus AD contrast. There was a high degree of overlap in the MCI and AD groups, with only one region of significantly decreased FA in the AD group that was not demonstrated in the NC versus MCI contrast. The one unique region of decreased FA in the NC versus AD comparison was in the posterior cingulate sub-

gyral white matter (voxel size = 11, Z score = 3.07, Talairach coordinates x : 16, y : -4, z : 46).

5. Discussion

In the present study we characterized in vivo changes in normal-appearing white matter microstructural integrity of participants with MCI and mild AD using whole brain diffusion tensor imaging. We found significant regional decreases of white matter anisotropy in the two patient groups compared to age-matched healthy controls in voxel-by-voxel comparisons. While no differences in regional molecular diffusion variables were detected between the MCI and mild AD groups, the anatomical pattern of white matter anisotropy changes (FA) was similar for both patient groups with greater posterior than anterior involvement. Moreover, decreases in posterior FA were not due to differential age or gender distributions among the groups, increased cardiovascular risk factors (e.g., diabetes, myocardial infarct, hypertension) in the cognitively impaired groups, or differential volume sizes of the DTI measures.

Our results are consistent with those of previous studies demonstrating impaired white matter integrity in MCI and AD using diffusion weighted MRI. The published findings have been based on both diffusion weighted imaging [16,36,37,46,65], which does not develop a full tensor and is, thus, susceptible to artifacts from differential head positions, and diffusion tensor imaging [15,33,39,64,68,74], a technique that is invariant to head position. Most of the published studies on MCI and AD have inferred impaired white matter integrity from findings of both increased free-molecular diffusion (mean diffusivity) and decreased directional diffusion (anisotropic diffusion), although some studies have only reported increases in free-molecular diffusion [36,39,46] or have failed to find any significant differences [16].

Diffusion weighted and diffusion tensor imaging studies have demonstrated various regional abnormalities of white matter integrity in patients with MCI and AD. The location of these anomalies differs across studies depending upon the exact placement of the ROIs. For example, some studies have investigated limited regions such as the corpus callosum [36], posterior cingulum [74], or temporal lobe regions [37], but others have investigated multiple ROIs in the frontal lobes, temporal lobes, cingulum, parietal lobes, and occipital lobes [15,16,33,39,46,64,65,68]. The most consistent findings across studies are of impaired white matter integrity in the corpus callosum, temporal lobe, parietal lobe, and the cingulum, with greater posterior than anterior involvement [39,65,68].

The variability of previous results may be due to multiple factors. These factors could include effects of different head positions in those studies that did not develop a position-invariant tensor, inclusion of MCI with mixed cognitive domain impairments, and/or differential placement of ROIs across studies. In contrast to these potential influences

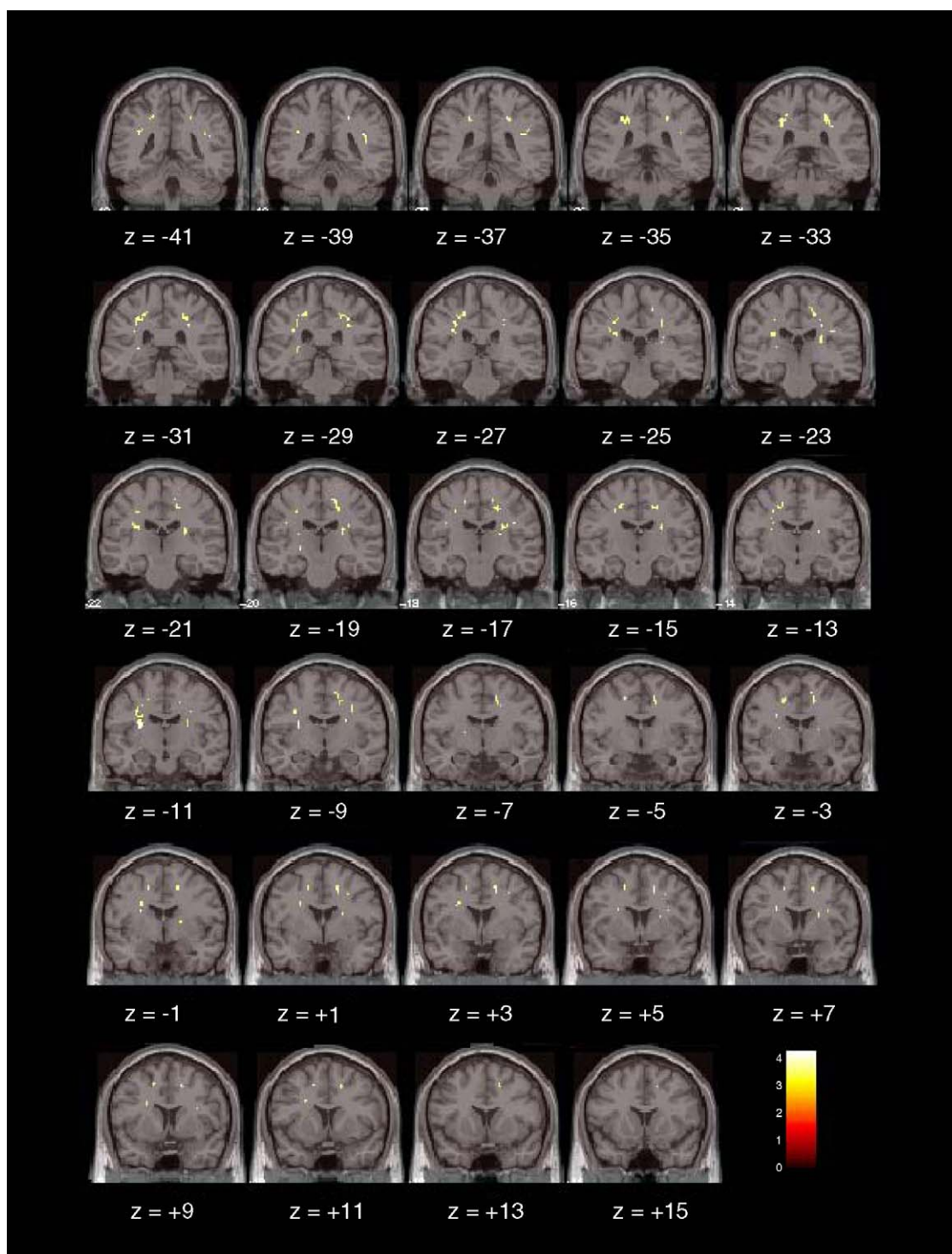


Fig. 2. Representative regions of significantly reduced fractional anisotropy (FA) in patients with Alzheimer's disease (AD) compared to age-matched healthy control participants. Three dimensional volumes were created from contiguous individual slices and normalized to a common standardized brain volume using SPM99 [35]. Differences were analyzed using a two-sample t -test statistic. Significance thresholds were set for $p < 0.01$. Voxels evidencing significant differences between groups are displayed on representative coronal sections on a canonical brain image. The color scale indicates the magnitude of Z values with lowest appearing in dark red and the highest in bright yellow/white. The left side of the images represents the left side of the brain.

on determination of anisotropic changes in MCI and AD, we developed position-invariant diffusion indexes derived from a full tensor, studied amnesic MCI only, and used a whole-brain voxel-based analytic method. Additionally, we

separated the 0 diffusion weighted images (T2 relaxation time) into CSF, gray matter and white matter segments. The WM segment image was then applied to each individual DW and FA maps to avoid "contamination" of the DW or FA maps

by elements other than white matter, such as hyperintensities, CSF, gray matter, and extra-cerebral matter. The exclusion of cortical gray matter decreases the potential artifact of echo planar distortions at brain/air/bone interfaces, most notable at the frontal pole and inferior temporal regions.

In our study, strikingly similar regions of decreased white matter integrity were found in the MCI and AD groups, with most regions of significantly decreased FA located posterior to the anterior commissure. The presence of these regional alterations in MCI that are shared by participants with AD are consistent with findings in volumetric studies of gray matter changes, in which specific patterns of mesial temporal atrophy are seen in both groups and can predict longitudinally the conversion from MCI to AD [27,29,47,48].

The present results demonstrate significantly decreased FA in the fasciculi of the cortico-thalamic and thalamo-cortical connections through the internal capsule (superior and posterior thalamic peduncles) in both MCI and AD compared to controls. Additionally, the white matter fibers located deep in the posterior white matter, such as the superior longitudinal fasciculus and the posterior cingulum bundle, were particularly affected in patients with AD and MCI compared to controls. Indeed, the only region showing decreased white matter integrity unique to the AD group was in the posterior cingulum bundle.

Specific interest has been given to the cingulum bundle in DTI investigations of WM integrity in patients with AD because of the existing evidence of the early involvement of the posterior cingulate in the progression of the disease. Neuropathological, MRI-volumetric [21], and especially brain metabolism studies [56,62,63,71] have indicated that the posterior cingulate is involved very early in the course of AD. Moreover, behavioral measures of mental status are significantly correlated with DTI-based diffusion values in the posterior cingulate gyrus among patients with AD [74].

The underlying white matter pathway of the cingulate gyrus is an important part of the cholinergic system [66]. Alterations of the cholinergic system in AD results from the loss of neurons of the nucleus basalis of Meynert (nbM), with a subsequent depletion of cortical acetylcholine and cholinergic fibers [54,55]. Additionally, a significant relationship between the presence of WMH in the cholinergic pathways and level of cognitive impairment has been reported with the severity of WMH in cholinergic fibers accounting for a specific impairment in executive functions, regardless of an equivalent global cognitive impairment rating [67]. Thus, our finding of decreased FA in the cingulum bundles in MCI and AD compared to NC could reflect increased vulnerability of this cortical cognitive system to damage of cholinergic pathways in incipient AD, as well as progressive damage in this region in those with AD.

The alterations in the microstructural integrity of normal-appearing WM in AD and MCI found in the present study may represent a complex result of co-existing pathological processes. One pathological process contributing to decreased

anisotropy in cortico-cortical and subcortico-cortical white matter tracts may be the presence of subclinical ischemic changes. Vascular risk factors and ischemic events, common in the elderly population, are known to increase the risk of AD [44]. As indicated in the introduction, alterations in microvasculature are commonly seen in brains of patients with AD [45]. In addition, there may be white matter rarefaction with axonal damage and gliosis [31]. In the present study however, the occurrence of clinically relevant cardiovascular risk factors (e.g., diabetes, myocardial infarct, hypertension) was similar across the three groups.

Another pathological process contributing to the loss of white matter integrity in MCI and AD may be increased susceptibility of oligodendrocytes to free-radical and other metabolic damage [4]. According to this theory, later myelinated regions (cortical association areas) have fewer oligodendrocytes supporting greater numbers of axons compared to earlier myelinated regions (primary cortical regions). Because of the high metabolic demands of oligodendrocytes in the cortical association areas needed to maintain the widely distributed axons, formation of ferritin-released iron is increased and may amplify pathological processes due to oxidative stress. These, and other metabolic processes may lead to decreased white matter integrity in association cortical regions due to damage to the supporting oligodendrocytes. In general, our findings of decreased white matter integrity in later-myelinating regions in patients with MCI and AD support this hypothesis.

In the early stages of AD, there is increased gray matter pathology in posterior brain regions relative to anterior regions [1,17]. Our finding of decreased posterior DTI indices of white matter integrity in MCI and early AD demonstrates that this pathological process occurs in white matter as well. The white matter changes in the cognitively impaired groups are independent of the presence of cardiovascular risk factors such as diabetes, myocardial infarct or hypertension and cannot be accounted for by differences in age distributions between the groups. Therefore, our results suggest that posterior white matter damage is specific to the pathological processes of AD. The occurrence of significant regional changes of whole brain WM anisotropy in both MCI and AD groups, compared to controls, suggests that posterior regional anisotropy changes in normal-appearing white matter of patients with MCI could occur before the onset of overt dementia and may play a role in the progression towards AD.

Acknowledgement

We thank all participants for their enthusiastic support of our efforts and for their diligence in complying with the evaluations. We also thank the staff of the RADC clinic, especially Barbara Eubler, for an outstanding job in recruiting participants in the study, and the reviewers for their insightful comments on an earlier draft of the paper.

References

- [1] Arnold SE, Hyman BT, Flory J, Damasio AR, Van Hoesen GW. The topographical and neuroanatomical distribution of neurofibrillary tangles and neuritic plaques in the cerebral cortex of patients with Alzheimer's disease. *Cereb Cortex* 1991;1:103–16.
- [2] Barber R, Scheltens P, Gholkar A, Ballard C, McKeith I, Ince P, et al. White matter lesions on magnetic resonance imaging in dementia with Lewy bodies, Alzheimer's disease, vascular dementia, and normal aging. *J Neurol Neurosurg Psychiatr* 1999;67:66–72.
- [3] Baron JC, Chetelat G, Desgranges B, Percey G, Landeau B, de la Sayette V, et al. In vivo mapping of gray matter loss with voxel-based morphometry in mild Alzheimer's disease. *Neuroimage* 2001;14:298–309.
- [4] Bartzokis G. Age-related myelin breakdown: a developmental model of cognitive decline and Alzheimer's disease. *Neurobiol Aging* 2004;25:5–18.
- [5] Bartzokis G, Cummings JL, Sultzer D, Henderson VW, Nuechterlein KH, Mintz J. White matter structural integrity in healthy aging adults and patients with Alzheimer's disease. *Arch Neurol* 2003;60:393–8.
- [6] Bartzokis G, Sultzer D, Lu PH, Nuechterlein KH, Mintz J, Cummings JL. Heterogenous age related breakdown of white matter structural integrity: implications for cortical "disconnection" in aging and Alzheimer's disease. *Neurobiol Aging* 2004;25:843–51.
- [7] Basser PJ. Inferring microstructural features and the physiological state of tissues from diffusion-weighted images. *NMR Biomed* 1995;8:333–44.
- [8] Basser PJ, Matiello J, Le Bihan D. Estimation of the effective self-diffusion tensor from the NMR spin echo. *J Magn Reson B* 1994;103:247–54.
- [9] Basser PJ, Pierpaoli C. Microstructural and physiological features of tissues elucidated by quantitative-diffusion-tensor MRI. *J Magn Reson B* 1996;111:209–19.
- [10] Bennett DA. Mild cognitive impairment. *Clin Geriatr Med* 2004;20:15–25.
- [11] Bennett DA, Wilson RS, Schneider JA, Evans DA, Mendes de Leon CF, Arnold SE, et al. Education modifies the relation of AD pathology to level of cognitive function in older persons. *Neurology* 2003;60:1909–15.
- [12] Bigler ED, Kerr B, Victoroff J, Tate DF, Breitner JCS. White matter lesions, quantitative magnetic resonance imaging, and dementia. *Alzheimer Dis Assoc Disord* 2002;16:161–70.
- [13] Bobinski M, de Leon MJ, Convit A, De Santi S, Wegiel J, Tarshish CY, et al. MRI of entorhinal cortex in mild Alzheimer's disease. *Lancet* 1999;353:38–40.
- [14] Bowen J, Teri L, Kukull W, McCormick W, Mc Curry SM, Larson EB. Progression to dementia in patients with isolated memory loss. *Lancet* 1997;349:763–5.
- [15] Bozzali M, Falini A, Franceschi M, Cercignani M, Zuffi M, Scotti G, et al. White matter damage in Alzheimer's disease assessed in vivo using diffusion tensor magnetic resonance imaging. *J Neurol Neurosurg Psychiatr* 2002;72:742–6.
- [16] Bozzao A, Floris R, Baviera ME, Apruzzese A, Simoneti G. Diffusion and perfusion MR imaging in cases of Alzheimer's disease: correlations with cortical atrophy and lesion load. *Am J Neuroradiol* 2001;22:1030–6.
- [17] Braak H, Braak E. Staging of Alzheimer's disease-related neurofibrillary changes. *Neurobiol Aging* 1995;16:271–8.
- [18] Bronge L, Bogdanovic N, Wahlund LO. Postmortem MRI and histopathology of white matter changes in Alzheimer brains. *Dement Geriatr Cogn Disord* 2002;13:205–12.
- [19] Brun A, Englund E. A white matter disorder in dementia of the Alzheimer type: a pathoanatomical study. *Ann Neurol* 1986;19:253–62.
- [20] Busatto GF, Garrido GEJ, Almeida OP, Castro CC, Camargo CHP, Cid CG, et al. A voxel-based morphometry study of temporal lobe gray matter reductions in Alzheimer's disease. *Neurobiol Aging* 2003;24:221–31.
- [21] Callen DJA, Black SE, Gao F, Caldwell CB, Szalai JP. Beyond the hippocampus. MRI volumetry confirms widespread limbic atrophy in AD. *Neurology* 2001;57:1669–74.
- [22] Convit A, de Leon MJ, Tarshish C, De Santi S, Tsui W, Rusinek H, et al. Specific hippocampal volume reductions in individuals at risk for Alzheimer's disease. *Neurobiol Aging* 1997;18:131–8.
- [23] Daly E, Zaitchik D, Copeland M, Schmahmann J, Gunther J, Albert M. Predicting conversion to Alzheimer's disease using standardized clinical information. *Arch Neurol* 2000;57:675–80.
- [24] DeCarli C, Miller BL, Swan GE, Reed T, Wolf PA, Carmelli D. Cerebrovascular and brain morphologic correlates of mild cognitive impairment in the National Heart, Lung, and Blood Institute Twin Study. *Arch Neurol* 2001;58:643–7.
- [25] de Crespigny AJ, Moseley ME. Eddy current induced image warping in diffusion weighted EPI. In: *Proceedings of the ISMRM sixth meeting*. 1998. p. 661.
- [26] deToledo-Morrell L, Goncharova I, Dickerson B, Wilson RS, Bennett DA. From healthy aging to early Alzheimer's disease: in vivo detection of entorhinal cortex atrophy. *Ann NY Acad Sci* 2000;911:240–753.
- [27] deToledo-Morrell L, Stoub TR, Bulgakova M, Wilson RS, Bennett DA, Leurgans S, et al. MRI-derived entorhinal volume is a good predictor of conversion from MCI to AD. *Neurobiol Aging* 2004;25:1197–203.
- [28] deToledo-Morrell L, Sullivan MP, Morrell F, Wilson RS, Bennett DA, Spencer S. Alzheimer's disease: In vivo detection of differential vulnerability of brain regions. *Neurobiol Aging* 1997;18:438–63.
- [29] Dickerson BC, Goncharova I, Sullivan MP, Forchetti C, Wilson RS, Bennett DA, et al. MRI-derived entorhinal and hippocampal atrophy in incipient and very mild Alzheimer's disease. *Neurobiol Aging* 2001;22:747–54.
- [30] Du AT, Schuff N, Amend D, Laakso MP, Hsu YY, Jagust WJ, et al. MRI of entorhinal cortex and hippocampus in mild cognitive impairment and Alzheimer's disease. *J Neurol Neurosurg Psychiatr* 2001;71:441–7.
- [31] Englund E. Neuropathology of white matter changes in Alzheimer's disease and vascular dementia. *Dement Geriatr Cogn Disord* 1998;9(Suppl. 1):6–12.
- [32] Fazekas F, Kapeller P, Schmidt R, Offenbacher H, Payer F, Fazekas G. The relation of cerebral magnetic resonance signal hyperintensities to Alzheimer's disease. *J Neurol Sci* 1996;142:121–5.
- [33] Fellgiebel A, Wille P, Muller MJ, Winterer G, Scheurich A, Vucurevic G, et al. Ultrastructural hippocampal and white matter alterations in mild cognitive impairment: a diffusion tensor imaging study. *Dement Geriatr Cogn Disord* 2004;18:101–8.
- [34] Folstein MF, Folstein SE, McHugh PR. "Mini-mental state". A practical method for grading the mental status of patients for the clinician. *J Psychiatr Res* 1975;12:189–92.
- [35] Friston KJ, Holmes AP, Worsley KJ, Poline JB, Frith JD, Frackowiak RS. Statistical parametric maps in functional imaging: a general linear approach. *Human Brain Map* 1995;2:189–210.
- [36] Hanyu H, Asano T, Sakurai H, Imon Y, Iwamoto T, Takasake M, et al. Diffusion-weighted and magnetization transfer imaging of the corpus callosum in Alzheimer's disease. *J Neurol Sci* 1999;167:37–44.
- [37] Hanyu H, Sakurai H, Iwamoto T, Takasaki M, Shindo H, Abe K. Diffusion weighted MR imaging of the hippocampus and temporal white matter in Alzheimer's disease. *J Neurol Sci* 1998;156:195–200.
- [38] Haselgrove JC, Moore JR. Correction for distortion of echo-planar images used to calculate the apparent diffusion coefficient. *Magn Reson Med* 1996;36:960–4.
- [39] Head D, Buckner RL, Shimony JS, Williams LE, Akbudak E, Conturo TE, et al. Differential vulnerability of anterior white matter in nondemented aging with minimal acceleration in dementia of the Alzheimer type: evidence from diffusion tensor imaging. *Cereb Cortex* 2004;4:410–23.

- [40] Hirono N, Kitagaki H, Kazui H, Hashimoto M, Mori E. Impact of white matter changes on clinical manifestation of Alzheimer's disease. *Stroke* 2000;31:2181–8.
- [41] Jack CR, Petersen RC, O'Brien PC, Tangalos EG. MR-based hippocampal volumetry in the diagnosis of Alzheimer's disease. *Neurology* 1992;42:183–8.
- [42] Jack CR, Petersen RC, Xu YC, Waring SC, O'Brien PC, Tangalos EG, et al. Medial temporal atrophy on MRI in normal aging and very mild Alzheimer's disease. *Neurology* 1997;49:786–94.
- [43] Jack CR, Shiung MM, Gunter JL, O'Brien PC, Weigand SD, Knopman DS, et al. Comparison of different MRI brain atrophy rate measures with clinical disease progression in AD. *Neurology* 2004;62:591–600.
- [44] Kaloria RN. The role of cerebral ischemia in Alzheimer's disease. *Neurobiol Aging* 2000;21:321–30.
- [45] Kaloria RN. Small vessel disease and Alzheimer's dementia: Pathological considerations. *Cerebrovasc Dis* 2002;13(Suppl 2):48–52.
- [46] Kantarci K, Jack CR, Xu YC, Campeau NG, O'Brien PC, Smith GE, et al. Mild cognitive impairment and Alzheimer's disease: Regional diffusivity of water. *Radiology* 2001;219:101–7.
- [47] Killiany RJ, Gomez-Isla T, Moss M, Kikinis R, Sandor T, Jolesz F, et al. Use of structural magnetic resonance imaging to predict who will get Alzheimer's disease. *Ann Neurol* 2000;47:430–9.
- [48] Killiany RJ, Hyman BT, Gomez-Isla T, Moss MB, Kikinis R, Jolesz F, et al. MRI measures of entorhinal cortex vs hippocampus in preclinical AD. *Neurology* 2002;58:1188–96.
- [49] Kordower JH, Chu Y, Stebbins GT, DeKosky ST, Cochran EJ, Bennett DA, et al. Loss and atrophy of layer II entorhinal cortex neurons in elderly people with mild cognitive impairment. *Ann Neurol* 2001;49:202–13.
- [50] Lancaster JL, Woldorff MG, Parsons LM, Liotti M, Freitas CS, Rainey L, et al. Automated Talairach Atlas labels for functional brain mapping. *Human Brain Map* 2000;10:120–31.
- [51] Lopez OL, Becker JT, Rezek D, Wess J, Boller F, Reynolds CF, et al. Neuropsychiatric correlates of cerebral white-matter radiolucencies in probable Alzheimer's disease. *Arch Neurol* 1992;49:828–34.
- [52] Makris N, Worth AJ, Sorenson AG, Papadimitriou GM, Wu O, Reese TG, et al. Morphometry of in vivo human white matter association pathways with diffusion-weighted magnetic resonance imaging. *Ann Neurol* 1997;42:951–62.
- [53] McKhann G, Drachman D, Folstein M, Katzman R, Price D, Stadlan EM. Clinical diagnosis of Alzheimer's disease: report of the NINCDS/ADRDA work group under the auspices of the Department of Health and Human Services Task Force on Alzheimer's disease. *Neurology* 1984;34:939–44.
- [54] Mesulam M-M. The cholinergic innervation of the human cerebral cortex. *Prog Brain Res* 2004;145:67–78.
- [55] Mesulam M-M, Geula C. Nucleus basalis (Ch4) and cortical cholinergic innervation in the human brain: Observations based on the distribution of acetylcholinesterase and choline acetyltransferase. *J Comp Neurol* 1988;275:216–40.
- [56] Minoshima S, Giordani B, Berent S, Frey KA, Foster NL, Kuhl DE. Metabolic reduction in the posterior cingulate cortex in very early Alzheimer's disease. *Ann Neurol* 1997;42:85–94.
- [57] Morris JC, Heyman A, Mohs RC, van Belle G, Fillenbaum G, Mellits ED, et al. The Consortium to Establish a Registry for Alzheimer's Disease (CERAD). Part 1. Clinical and neuropsychological assessment of Alzheimer's disease. *Neurology* 1989;39:1159–65.
- [58] Mufson EJ, Chin EY, Cochran EJ, Beckett LA, Bennett DA, Kordower JH. Entorhinal cortex beta amyloid load in individuals with mild cognitive impairment. *Exp Neurol* 1999;158:469–90.
- [59] Petersen RC. Aging, mild cognitive impairment and Alzheimer's disease. *Neurol Clin* 2000;18:789–806.
- [60] Petersen RC, Doody R, Kurz A, Mohs RC, Morris JC, Rabins PV, et al. Current concepts in mild cognitive impairment. *Arch Neurol* 2001;58:1985–92.
- [61] Petersen RC, Smith GE, Waring SC, Ivnik RJ, Tangalos EG, Kokmen E. Mild cognitive impairment: clinical characterization and outcome. *Arch Neurol* 1999;56:303–8.
- [62] Reiman EM, Caselli RJ, Chen K, Alexander GE, Bandy D, Frost J. Declining brain activity in cognitively normal apolipoprotein E ϵ 4 heterozygotes: a foundation for using positron emission tomography to efficiently test treatments to prevent Alzheimer's disease. *Proc Natl Acad Sci USA* 2001;98:334–39.
- [63] Reiman EM, Caselli RJ, Yun LS, Chen K, Bandy D, Minoshima S, et al. Preclinical evidence of Alzheimer's disease in persons homozygous for the epsilon 4 allele for apolipoprotein E. *N Engl J Med* 1996;334:752–8.
- [64] Rose SE, Chen F, Chalk JB, Zelaya FO, Strugnell WE, Benson M, et al. Loss of connectivity in Alzheimer's disease: an evaluation of white matter tract integrity with color coded MR diffusion tensor imaging. *J Neurol Neurosurg Psychiatr* 2000;69:528–30.
- [65] Sandon TA, Felician O, Edelman RR, Warach S. Diffusion weighted magnetic resonance imaging in Alzheimer's disease. *Dementia* 1999;10:166–71.
- [66] Selden NR, Gitelman DR, Salamon-Murayama N, Parrish TB, Mesulam MM. Trajectories of cholinergic pathways within the cerebral hemispheres of the human brain. *Brain* 1998;121:2249–57.
- [67] Swartz RH, Sahlas DJ, Black SE. Strategic involvement of cholinergic pathways and executive dysfunction: Does location of white matter signal hyperintensities matter? *J Stroke Cerebrovasc Dis* 2003;12:29–36.
- [68] Takahashi S, Yonezawa H, Takahashi J, Kudo M, Inoue T, Toghi H. Selective reduction of diffusion anisotropy in white matter of Alzheimer's disease brains measured by 3.0 Tesla magnetic resonance imaging. *Neurosci Lett* 2002;332:45–8.
- [69] Talairach J, Tournoux P. Co-planar stereotaxic atlas of the human brain. New York: Thieme Medical Publishers; 1988.
- [70] Ulug A, Moore DF, Bojko AS, Zimmerman RD. Clinical use of diffusion-tensor imaging for diseases causing neuronal and axonal damage. *Am J Neuroradiol* 1999;20:1044–8.
- [71] Valla J, Berndt JD, Gonzalez-Lima F. Energy hypometabolism in posterior cingulate cortex of Alzheimer's patients: superficial laminar cytochrome oxidase associated with disease duration. *J Neurosci* 2001;13:4923–30.
- [72] Wilson RS, Sullivan MP, deToledo-Morrell L, Stebbins GT, Bennett DA, Morrell F. Association of memory and cognition in Alzheimer's disease with volumetric estimates of temporal lobe structures. *Neuropsychology* 1996;10:459–63.
- [73] Xu Y, Jack CR, O'Brien PC, Kokmen E, Smith GE, Ivnik RJ, et al. Usefulness of MRI measures of entorhinal cortex versus hippocampus in AD. *Neurology* 2000;54:1760–7.
- [74] Yoshiura T, Mihara F, Ogomori K, Tanaka A, Kaneko K, Masuda K. Diffusion tensor in posterior cingulate gyrus: correlation with cognitive decline in Alzheimer's disease. *Neuroreport* 2002;13:2299–302.